JMSAE
journal of Materials Science and Applied Energy

P. Masakul et al. / J. Mater. Sci. Appl. Energy. 11(3) (2022) 245716

The effect of Mn-doping on dielectric properties of titanate nanowires

Pristanuch Masakul[a,*], Prasit Thongbai[b], Santi Maensiri[c]

[a] Department of Applied Physics, Faculty of Sciences and Liberal Arts, Rajamangala University of Technology Isan, Nakhon Ratchasima, 30000 Thailand
[b] Department of Physics, Faculty of Science, Khon Kaen University, Khon Kaen, 40002 Thailand
[c] School of Physics, Institute of Science Suranaree University of Technology, Nakhon Ratchasima, 30000 Thailand

***Corresponding Author:** pristanuch.ka@rmuti.ac.th
https://doi.org/10.55674/jmsae.v11i3.245716

Received: 28 September 2021 | **Revised:** 24 November 2021 | **Accepted:** 31 August 2022 | **Available online:** 1 September 2022

Abstract

Mn-doped titanate nanowires (TNWs) with system of $Mn_xTi_{3-x}O_7$ ($Na_{0.96}H_{1.04}$·$3.42H_2O$) (where x = 0, 0.05, 0.10, 0.20, and 0.30) were fabricated a hydrothermal route at 130 °C for 24 h. The products were investigated by X-ray diffraction (XRD), scanning electron microscopy (SEM), and UV-vis spectroscopy. The nanowires were an average diameter of about 10–50 nm and an average range length of micrometer scales. The dielectric relaxation in the $Mn_xTi_{3-x}O_7$ ($Na_{0.96}H_{1.04}$·$3.42H_2O$) system was determined by LCR Meter in difference frequency (10^2–10^6 Hz) at various temperatures. The Mn-doped TNWs samples showed a giant dielectric exhibit with a dielectric constant of about 10^4 at 30 °C and 1 kHz. They all have a Debye-like relaxation based on the Maxwell-Wagner polarization. The dielectric constant of Mn-doped TNWs significantly increased with increasing doping levels.

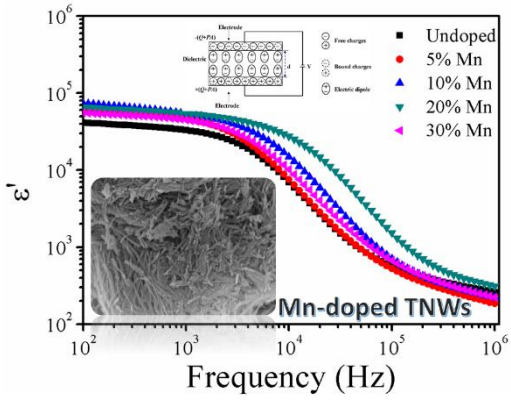

Keywords: Titanate nanowires; Dielectric properties; Mn-doped TNWs.

© 2022 Center of Excellence on Alternative Energy reserved

Introduction

In the last decades, high dielectric constant ferroelectric ceramics such as $BaTiO_3$ [1] and $PbMg_{1/3}Nb_{2/3}O_3$ have been studies intensively [2]. The $CaCu_3Ti_4O_{12}$ ceramic has a perovskite-like oxide structure, which exhibits a ε' of about 10^5 over a wide temperature range from room temperature to 300 °C [3, 4]. In recent years, it was reported that titanate nanotubes (TNTs) showed a ε' of about 10^4 – 10^6 at low frequency [5 – 7]. The dielectric relaxation of TNTs base was related to associated with their high grain conductivity, which is the important factor contributing to the Maxwell-Wagner polarization mechanism. Kasian et al. [6], have added different contents of Co doping ions into TNTs with 5 – 40% and studied the dielectric properties of Co-doped TNTs. After doping TNTs with Co ions, the ε' increased and tanδ significantly decreased. Replacing the precious metal with a more common metal in TNTs can be significantly improve dielectric properties. Among these dopants, Mn has been reported to improve dielectric response and sinterability in a certain extent due to the modification of mixed valent structure. The addition of Mn^{2+} can reduce dielectric losses and increase the densification of dielectric metals [24]. In addition, Mn^{2+} substitution into BZT can reduce tanδ to be less than 0.02 [25].

In this paper, we successfully prepared Mn-doped TNWs by a hydrothermal route at the temperature of 130 °C for 24 h. The effects of Mn doping ions on the dielectric properties of TNWs were studied and discussed in detail.

Materials and Methods

Mn-doped TNWs were prepared by a hydrothermal process using anatase-TiO_2, MnN_2O_6·xH_2O and NaOH. Typically, TiO_2 and MnN_2O_6·xH_2O were calculated according to the stoichiometric composite $A_2(Ti_{3-x}Mn_x)O_7$·nH_2O (A_2=$Na_{0.036}$ $H_{1.964}$)(where x = 0, 0.05, 0.10, 0.20 and 0.30). The precursor was dissolved in 160 ml of NaOH (10M) mixture solution under magnetic stirring for 24 h and followed by ultrasonic for 2h. The product was transferred into a Teflon-line autoclave and sealed. After

reaction at 130 °C for 24 h, the autoclave was cooled to room temperature. Then, the product was washed using de-ionized water several times until the pH was closed to 7 and dried at 70 °C in oven. The crystal structure of Mn-doped TNWs were characterized by X-ray diffraction (XRD) using CuKα radiation with λ = 0.154060 nm (D2, Bruker, Germany). The microstructure of prepared Mn-doped TNWs was characterized by scanning electron microscopy (FE-SEM, Carl Zeiss, Auriga). Absorption of Mn-doped TNWs was investigated by UV-Vis spectroscopy (Shimadzu UV-3101PC). For dielectric measurements, electrodes were painted with silver paste and dried at 70 °C for 5 min. The dielectric properties were determined by using a Keysight E4990A precision LCR meter as functions of frequency (10^2 – 10^6 Hz) and temperature (-60 – 200 °C) at oscillation voltage of 0.50 V.

Results and Discussion

Fig. 1 presents the XRD results for Mn-doped TNWs. The results indicated that a single phase with monoclinic trititanate ($H_2Ti_3O_7$, JCPDF 47-0561) was detected in all samples [8, 9]. For Mn-doped TNWs, as the Mn doping concentration increases and there was a decrease in the intensity of the peaks. This is attributed to the effects caused in the substitute of the Ti^{4+} ions (0.68 Å) by Mn^{2+} ions (0.70 Å) into the TNWs lattice [10, 11]. It was ascribed that this phenomenon may be caused by the distortion of crystalline order within the layers due to the ion-exchange [11]. Consequently, the deformation of crystal lattice, which resulted in a decrease in the crystallite size as clearly indicated by the broadening peak and decreasing peak intensity. The optical absorbance was measured by UV-Vis spectroscopy (Fig. 2). The absorption peaks could be rather divided into 2 groups. The first one is 5% Mn and 20% Mn, their peak intensities reduced and shifted to the red. The second group is an undoped, 10% Mn, and 30% Mn, their peak intensities were higher than the first group and seemed to stay still at the same position, did not show the red shift. This can be understood as when the doping concentration is high, the inconsistency in precipitation may lead the dopants to form clusters. All the Mn-doped TNTs displayed moderate absorbance in the visible light region in the range of 400 – 800 nm like previous reports [12]. The red shift associated with the manganese concentration increase, with the related mechanism of charge transfer within structure [10, 12 – 14]. The band gap (E_g) is the strength of the optical absorption, as presented in eq. (1) [10, 15]:

$$\alpha h\nu = A(h\nu - E_g)^2 \quad (1)$$

where α is the absorption coefficient, h is the Planck constant, ν is the photon's frequency, A is a proportionality constant and E_g is the energy band gap energy. The band gaps applied of all the samples is shown in Table 1.

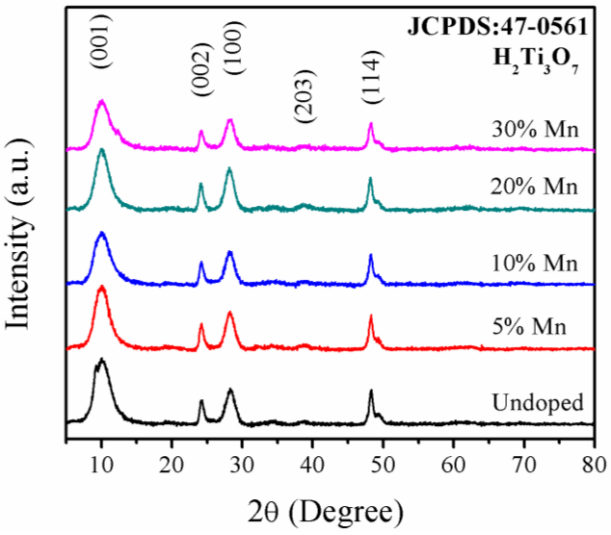

Fig. 1 XRD patterns of Mn-doped TNWs with different concentrations of Mn doping ions.

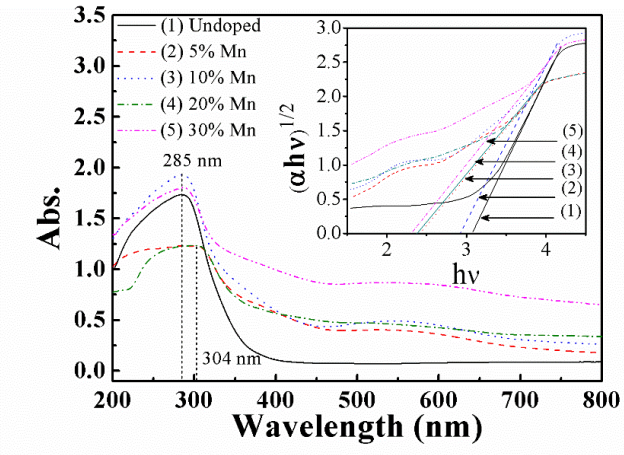

Fig. 2 UV–vis absorption spectra of samples obtained at room temperature.

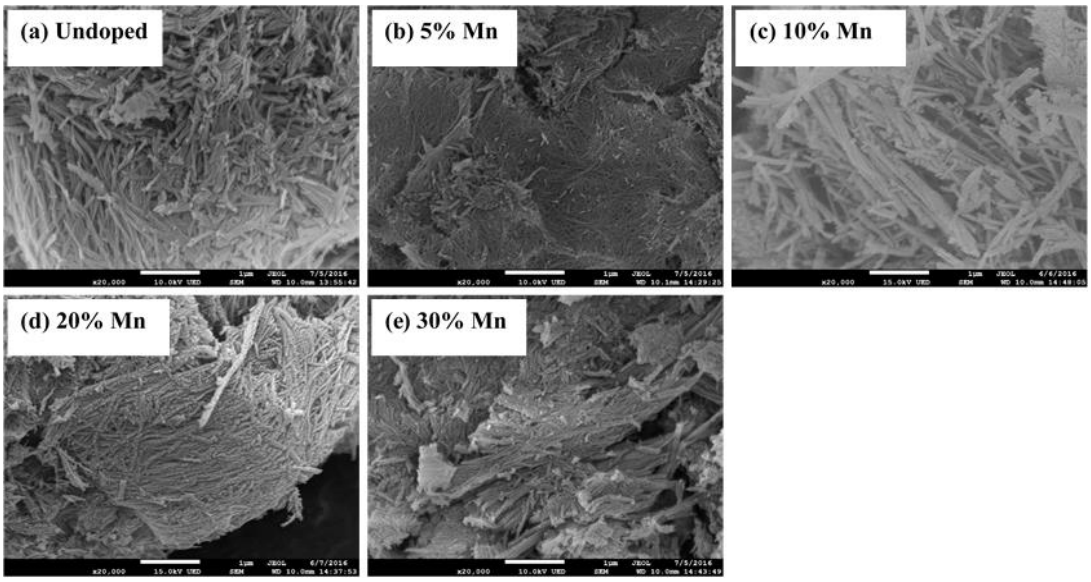

Fig. 3 SEM images of (a) undoped, (b) 5% Mn, (c) 10% Mn, (d) 20% Mn and (e) 30% Mn.

Fig. 3 shows SEM images of Mn-doped TNWs, all products exhibited both nanowire-like structures and particles. The average diameter of nanowires was ~10 – 50 nm and the length of the nanowires is about micrometers scales. The ε' of the Mn-doped TNWs was calculated from the capacitance value using the following eq. (2)

$$\varepsilon' = \frac{Cd}{\varepsilon_0 A} \tag{2}$$

where C is capacitance using the material as the dielectric capacitor, d the thickness of the sample, A the area of the plate, and ε_0 the permittivity of the free space, respectively. Figs. 4(a) – (d). illustrate the frequency dependence of dielectric properties of Mn-doped TNWs. As seen in Fig. 4(a), the ε' increases with increasing Mn^{2+} content (x = 0.05 – 0.20) to reach the maximum value of 5.50×10^4 at x = 0.20 (30 °C and 1 kHz) and then decreases with increasing Mn^{2+} content (x = 0.30). This may be due to the amount of Mn doping leading to lower carrier mobility. Some other previous works also reported that Mn doping has a significant influence on the dielectric property [17, 18]. Fig. 4(b) shows the tanδ response of various frequencies at temperature of 30 °C for undoped and Mn-doped TNWs. The low values of tanδ for all the samples are nearly independent of low frequency (10^2 – 10^3 Hz). All samples show the rapid increase in tanδ at high frequencies (>10^3 Hz). This is related to the dielectric relaxation process [19, 20].

Fig. 4(c) shows the influence of the Mn^{2+} doping on electrical properties of Mn-doped TNWs, which was characterized using impedance spectroscopy. Fig. 4(c) two semicircular arcs is found in these complex plots. This is attributed to the resistance of the insulating grain boundary (R_{gb}) and the resistance of the grain (R_g) (as show inset (1)) [21, 22]. It is observed that R_{gb} value is much larger than R_g value for all the sample. This result clearly indicates that the dielectric behavior in all samples should be correlated to the interfacial polarization or Maxwell-Wagner Polarization. Under an applied electric field, free charges in the semiconducting part were accumulated at the insulating interface, producing the strong interfacial polarization. The diameter of each semicircular arcs for both of the grain and grain boundary responses, tends to decrease with increase doping concentration. This result indicates that the Mn^{2+} doping affects the properties of TNWs by two possible apart from, i.e., substitution into lattice and formation of an impurity phase, with effect on the electrical properties of Mn-doped TNWs. The effect of temperature on dielectric properties is shown in Fig. 4(d). The tends to increase with increasing temperature. However, when the temperature higher than 120 °C, the ε' decreases with increasing temperatures. This can be explained that the structure of nanotubes was destroyed and changed into particles with increasing temperature, leading to decreases in ε'.

Table 1 Shows the dielectric constant (ε'), loss tangent (tanδ) (at 30 °C and 10 kHz), and energy gap (E_g) of Mn-doped TNWs.

Doping Level	ε'	tanδ	E_g(eV)
x = 0	4.10×10^4	0.40	3.10
x = 0.05	4.70×10^4	0.30	2.44
x = 0.10	5.40×10^4	0.30	2.92
x = 0.20	5.50×10^4	0.20	2.38
x = 0.30	4.50×10^4	0.30	2.31

The semicircles diameter of the sample decreased as the increasing temperature, confirming the semiconductor-like behavior of these materials [23] (see in Fig. 4(c); inset (2)). The effect of temperature on dielectric properties is shown in Fig. 4(d). This result suggests that the addition of Mn doping the increase of the ε' with the increase temperature. This dielectric exhibit is related to the dc conductivity [19]. The peak of ε' decreases as increasing of temperatures (>120 °C). These affect the structure of nanowires was destroyed and transformed into particles, leading to decreases in ε'.

Conclusion

The Mn-doped TNWs were sucessfully synthesized by a hydrothermal route. All the samples shown high dielectric behavior with a dielectric constant of about 10^4. The dielectric response have been explained on the basis of the Maxwell-Wagner polarization mechanism. The increase in ε' with Mn^{2+} doping was due to the increase in space charge carriers or interfacial polarization. An increase in the dielectric constant was thought to be the main cause for the improvement of both R_{gb} and R_g of the TNWs.

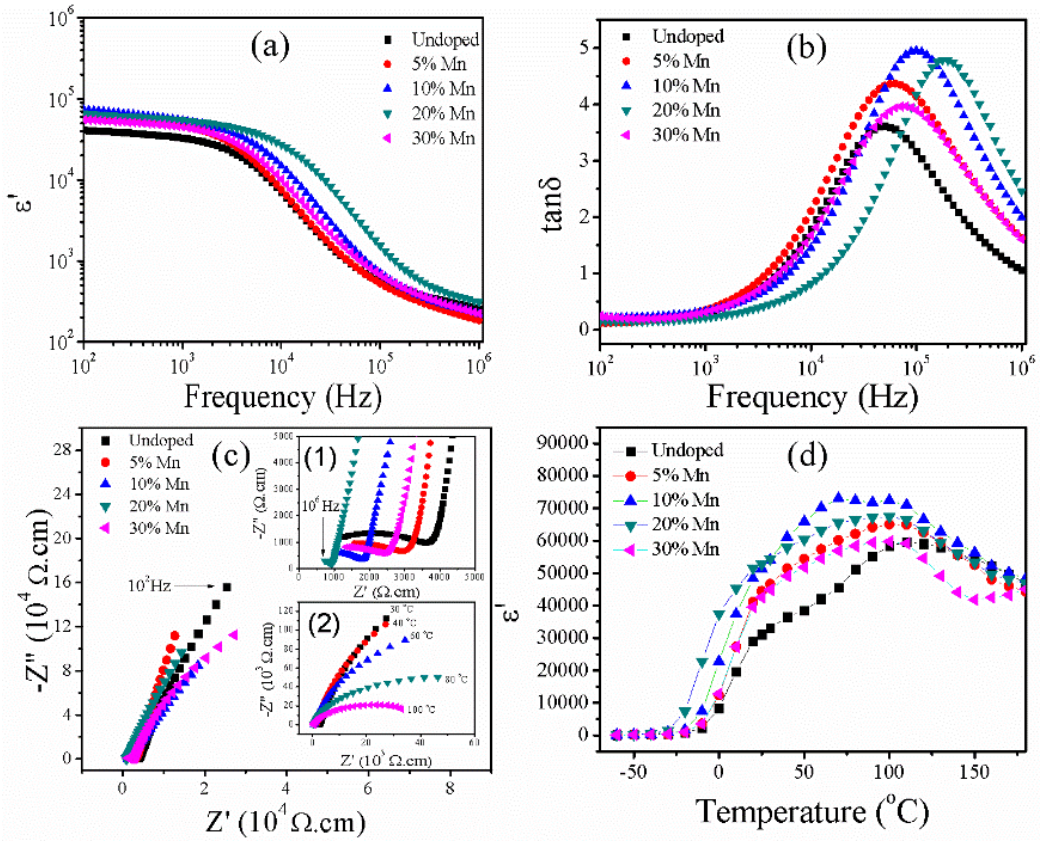

Fig. 4 Frequency dependence of (a) ε', (b) tanδ, (c) impedance spectra of undoped and Mn-doped TNWs at 30 °C; inset (1) of (c) impedance spectra at high frequency, and inset (2) of (c) impedance spectra plot at difference temperatures for the 30% Mn doped TNWs sample and (d) the temperature dependence of the dielectric constant (ε') between -60 – 200 °C at the difference frequency (10^2 – 10^6 Hz).

Acknowledgement

The financial support provided by Thailand Research Fund (TRF). Scholar, Contract No. MRG6280103. The authors would like to thank Rajamangala University of Technology Isan for financial support. Suranaree University of Technology and Khon Kaen University.

References

[1] G. Schileo, L. Luisman, A. Feteira, M. Deluca, K. Reichmann, Structure–property relationships in $BaTiO_3$–$BiFeO_3$–$BiYbO_3$ ceramics, J. Eur. Ceram. Soc. 33(8) (2013) 1457 – 1468.

[2] R. Yimnirun, S. Ananta, P. Laoratanakul, Dielectric and ferroelectric properties of lead magnesium niobate–lead zirconate titanate ceramics prepared by mixed-oxide method, J. Eur. Ceram. Soc. 25(13) (2005) 3235 – 3242.

[3] M.A. Subramanian, D. Li, N. Duan, B.A. Reisner, A.W. Sleight, High Dielectric Constant in $ACu_3Ti_4O_{12}$ and $ACu_3Ti_3FeO_{12}$ Phases, J. Solid State Chem. 151(2) (2000) 323 – 325.

[4] A.E. Smith, T.G. Calvarese, A.W. Sleight, M.A. Subramanian, An anion substitution route to low loss colossal dielectric $CaCu_3Ti_4O_{12}$, J. Solid State Chem. 182(2) (2009) 409 – 411.

[5] W. Hu, L. Li, W. Tong, G. Li, Water-titanate intercalated nanotubes: fabrication, polarization, and giant dielectric property, Phys. Chem. Chem. Phys. 12(39) (2010) 12638 – 12646.

[6] K. Pristanuch, Y. Teerapon, T. Prasit, R. Saroj, Y. Rattikorn, M. Santi, Co-doped titanate nanotubes: Synthesis, characterization, and properties, Jpn. J. Appl. Phys. 53(6S) (2014) 06JG12.

[7] P. Kasian, P. Thongbai, T. Yamwong, S. Rujirawat, R. Yimnirun, S. Maensiri, The DC Bias Voltage Effect and Non-Linear Dielectric Properties of Titanate Nanotubes, J. nanosci. nanotech. 15(11) (2015) 9197 – 9202.

[8] W. Hu, L. Li, G. Li, J. Meng, W. Tong, Synthesis of Titanate-Based Nanotubes for One-Dimensionally Confined Electrical Properties, J. Phys. Chem. C. 113(39) (2009) 16996 – 17001.

[9] H.-H. Ou, S.-L. Lo, Review of titania nanotubes synthesized via the hydrothermal treatment: Fabrication, modification, and application, Separ. Purif. Tech. 58(1) (2007) 179 – 191.

[10] R. Yuan, B. Zhou, D. Hua, C. Shi, Enhanced photocatalytic degradation of humic acids using Al and Fe co-doped TiO_2 nanotubes under UV/ozonation for drinking water purification, J. Hazard. Mater. 262 (2013) 527 – 538.

[11] P. Szirmai, E. Horváth, B. Náfrádi, Z. Micković, R. Smajda, D.M. Djokić, K. Schenk, L. Forró, A. Magrez, Synthesis of Homogeneous Manganese-Doped Titanium Oxide Nanotubes from Titanate Precursors, J. Phys. Chem. C. 117(1) (2013) 697 – 702.

[12] S.N.R. Inturi, T. Boningari, M. Suidan, P.G. Smirniotis, Visible-light-induced photodegradation of gas phase acetonitrile using aerosol-made transition metal (V, Cr, Fe, Co, Mn, Mo, Ni, Cu, Y, Ce, and Zr) doped TiO_2, Appl. Catal. B Environ. 144 (2014) 333 – 342.

[13] J. Zhu, W. Zheng, B. He, J. Zhang, M. Anpo, Characterization of Fe–TiO_2 photocatalysts synthesized by hydrothermal method and their photocatalytic reactivity for photodegradation of XRG dye diluted in water, J. Mol. Catal. A Chem. 216(1) (2004) 35 – 43.

[14] H.-C. Liang, X.-Z. Li, Effects of structure of anodic TiO_2 nanotube arrays on photocatalytic activity for the degradation of 2,3-dichlorophenol in aqueous solution, J. Hazard. Mater. 162(2 – 3) (2009) 1415 – 1422.

[15] Y.L. Pang, A.Z. Abdullah, Effect of low Fe^{3+} doping on characteristics, sonocatalytic activity and reusability of TiO_2 nanotubes catalysts for removal of Rhodamine B from water, J. Hazard. Mater. 235–236 (2012) 326 – 335.

[16] S.M. Sze, Physics of semiconductor devices, Wiley, New York 2004.

[17] Z. Yuan, Y. Lin, J. Weaver, X. Chen, C. L. Chen, G. Subramanyam, J. C. Jiang, E. I. Meletis, Large dielectric tunability and microwave properties of Mn-doped (Ba,Sr)TiO_3 thin films, Appl. Phys. Lett. 87 (2005), 152901.

[18] J. Cai, Y.-H. Lin, B. Cheng, C.-W. Nan, Dielectric and nonlinear electrical behaviors observed in Mn-doped $CaCu_3Ti_4O_{12}$ ceramic, Appl. Phys. Lett. 91 (2007), 252905.

[19] J. Wu, C.W. Nan, Y. Lin, Y. Deng, Giant dielectric permittivity observed in Li and Ti doped NiO, Phys. Rev. Lett. 89 (2002) 30.

[20] P. Thongbai, T. Yamwong, S. Maensiri, Correlation between giant dielectric response and electrical conductivity of CuO ceramic, Solid State Commun. 147 (2008) 385 – 387.

[21] T. Putjuso, P. Manyum, R. Yimnirun, T. Yamwong, P. Thongbai, S. Maensiri, Giant dielectric behavior of solution-growth CuO ceramics subjected to dc bias voltage and uniaxial compressive stress, Solid State Sci. 13 (2011) 158 – 162.

[22] D.C. Sinclair, T.B. Adams, F.D. Morrison, A.R. West, One-step internal barrier layer capacitor, Appl. Phys. Lett. 80 (2002) 2153.

[23] P. Laokul, P. Thongbai, T. Yamwong, S. Maensiri, High Dielectric Permittivity and Maxwell-Wagner Polarization in Magnetic $Ni_{0.5}Cu_{0.3}Zn_{0.2}Fe_2O_4$ Ceramics, J. Supercond. Nov. Magn. 25 (2012) 1195 – 1201.

[24] P. Parjansri, K. Pengpat, G. Rujijanagul, T. Tunkasiri, U.S. Intatha, Eitssayeam Effects of Mn and Sr Doping on the Electrical Properties of Lead-Free 0.92BCZT-0.08BZT. Ceram. Ferroelectr. 458(1) (2014) 91 – 97.

[25] W. Cai, C. Fu, J. Gao, X. Deng, Effect of Mn doping on the dielectric properties of $BaZr_{0.2}Ti_{0.8}O_3$ ceramics, J. of Mater. Sci.: Mater. in Electro. 21(4) (2010) 317 – 325.